SUPPLEMENTAL FIGURES

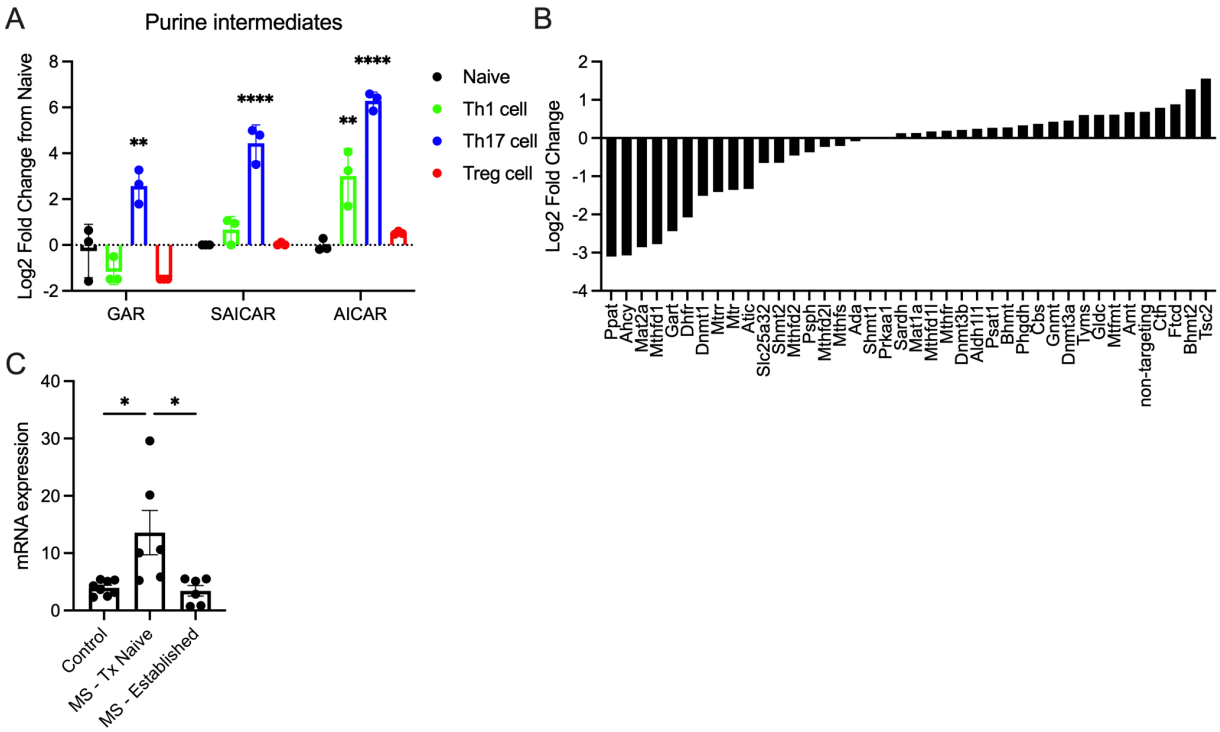

Figure S1: 1C metabolism and MTHFD2 expression in CD4⁺ T cells. Related to Figure 1.

(A) Change in concentrations of purine synthesis intermediates in differentiated CD4⁺ T cells compared to naïve measured by mass spectrometry (one-way ANOVA). (B) Change in gRNA abundance by gene from *in vivo* CRISPR screening (statistical analysis performed by MAGeCK, n=3). (C) MTHFD2 mRNA expression in whole blood of healthy controls, patients with treatment-naïve MS, and patients on treatment with disease remission (Aune et al., 2017) (mean±SEM, Kruskal-Wallis test).

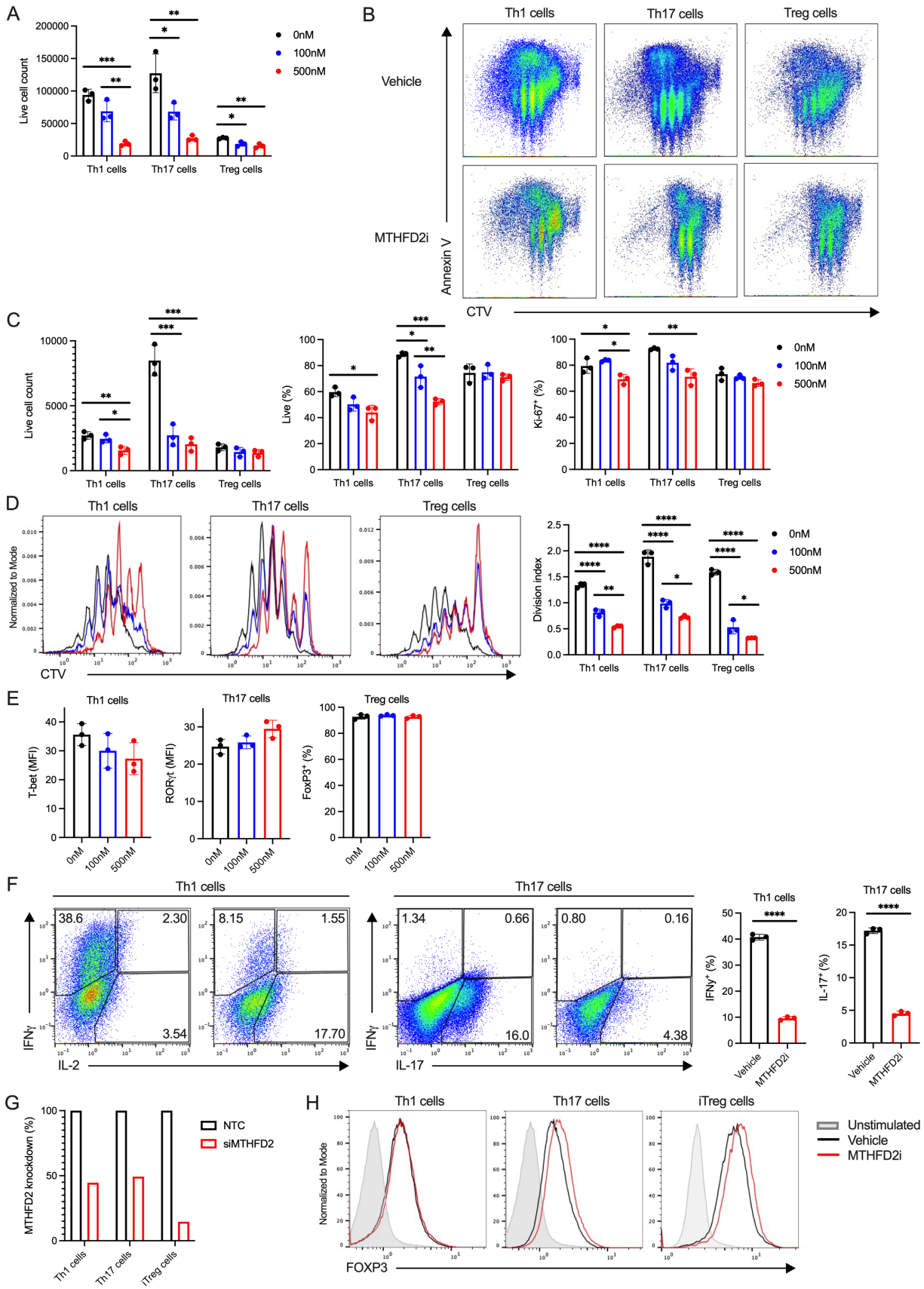
A
Live cell count
0nM
100nM
500nM
Th1 cells
Th17 cells
Treg cells
B
Th1 cells
Th17 cells
Treg cells
Vehicle
MTHFD2i
Annexin V
CTV
C
Live cell count
Live (%)
Ki-67+ (%)
D
Normalized to Mode
Division index
CTV
E
T-bet (MFI)
RORγt (MFI)
FoxP3+ (%)
F
IFNγ
IL-2
IL-17
IFNγ+ (%)
IL-17+ (%)
Vehicle
MTHFD2i
G
MTHFD2 knockdown (%)
NTC
siMTHFD2
iTreg cells
H
FOXP3
Unstimulated
Vehicle
MTHFD2i

Figure S2: $CD4^+$ T cell proliferation and function with early and delayed MTHFD2i treatment. Related to Figure 2 and Figure 4.

(A) Live cell count of $CD4^+$ T cells treated with MTHFD2i for 72hrs (one-way ANOVA). (B) CTV dilution and Annexin V staining in $CD4^+$ T cells treated with MTHFD2i for 72hrs (one-way ANOVA). Live (C) cell count, viability, Ki-67 expression, (D) CTV dilution, (E) TF expression in $CD4^+$ T cells activated for 24hrs and treated with MTHFD2i for 48hrs (one-way ANOVA). (F) Cytokine expression in Th1 and Th17 cells activated for 24hrs, treated with MTHFD2i for 72hrs, and stimulated with PMA and ionomycin for 4hrs (unpaired t-test). (G) qPCR measurement of MTHFD2 in human cells transduced with NTC or siMTHFD2. Data from one donor that is representative of four donors. (H) Representative flow cytometry profiles of data tabulated in Figure 4D showing FOXP3 expression in MTHFD2i-treated human $CD4^+$ T cells.

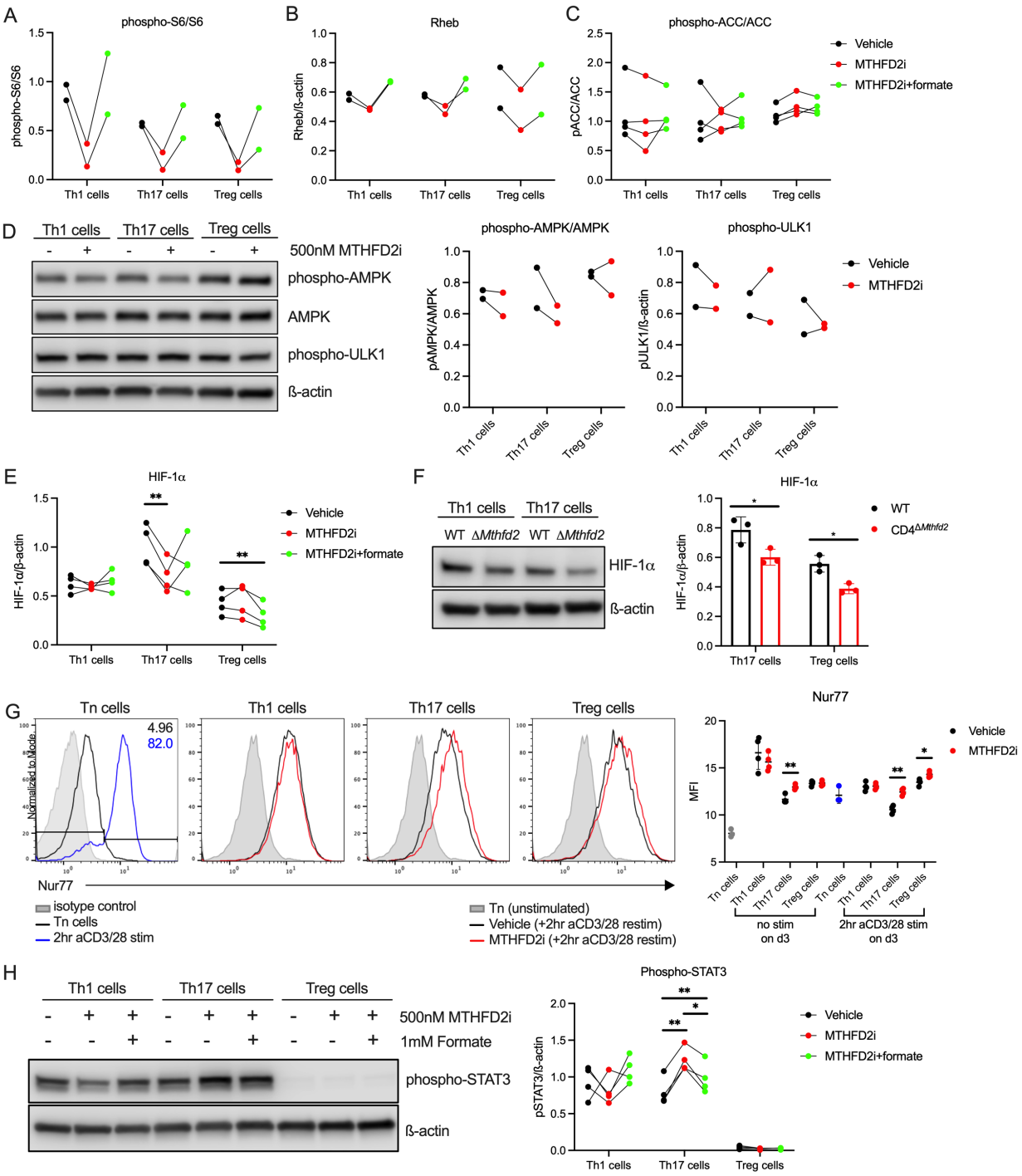

Figure S3: Altered Cell Signaling Upon MTHFD2i. Related to Figure 6.

Tabulation of band intensities from immunoblots for (A) phospho-S6/S6, (B) Rheb, and (C) phospho-ACC/ACC in CD4$^+$ T cells treated with vehicle, 500nM MTHFD2i or 500nM MTHFD2i+1mM formate for 72hrs (repeated measures one-way ANOVA). (D) Immunoblot of

phospho-AMPK/AMPK and phospho-ULK1 (Ser777) expression in $CD4^+$ T cells treated with MTHFD2i±formate for 72hrs (paired t-test). (E) Tabulated band intensities from immunoblots for HIF-1α in $CD4^+$ T cells treated with MTHFD2i±formate for 72hrs (repeated measures one-way ANOVA). (F) Immunoblot of HIF-1α expression in Th1 and Th17 cells from WT and $CD4^{\Delta Mthfd2}$ littermates activated and differentiated for 4 days (unpaired t-test). (G) Representative flow cytometry profiles and tabulated data for Nur77 expression in Tn, Th1, Th17, and Treg cells after 72hrs of culture with either vehicle or MTHFD2i and restimulated with anti-CD3 and anti-CD28 antibodies for 2hrs (unpaired t-test). (H) Immunoblot of phospho-STAT3 expression in $CD4^+$ T cells treated with MTHFD2i±formate for 72hrs (repeated measures one-way ANOVA).

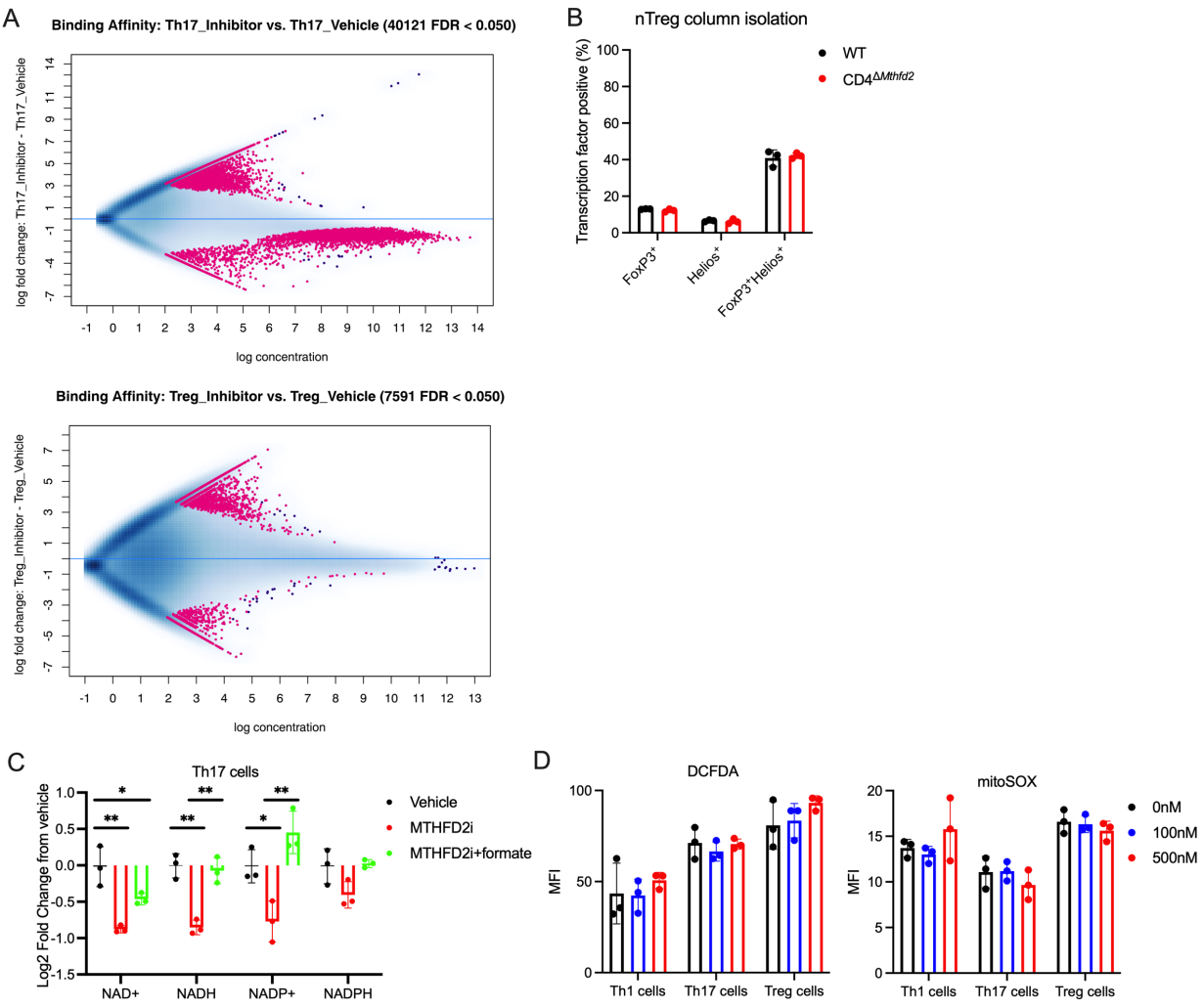

Figure S4: H3K27me3 in MTHFD2i-treated Th17 and Treg cells. Related to Figure 6.

(A) MA plot of H3K27me3 signal intensities measured by CUT&RUN in Th17 and Treg cells treated with vehicle or 500nM MTHFD2i. P-values obtained by Wald test and adjusted using Benjamini Hochberg's method. Pink indicates sites with significant differential modifications (FDR <0.05, n=3). (B) FoxP3 and Helios expression in cells isolated by CD25 positive selection column for nTreg cell purification (unpaired t-test). (C) Change in NAD^+, NADH, $NADP^+$, and NADPH in Th17 cells treated with MTHFD2i±formate for 6hrs relative to vehicle measured by mass spectrometry (one-way ANOVA). (D) Total cellular ROS (DCFDA) and mitochondrial superoxide (mitoSOX) levels in $CD4^+$ T cells treated with MTHFD2i for 72hrs (one-way ANOVA).

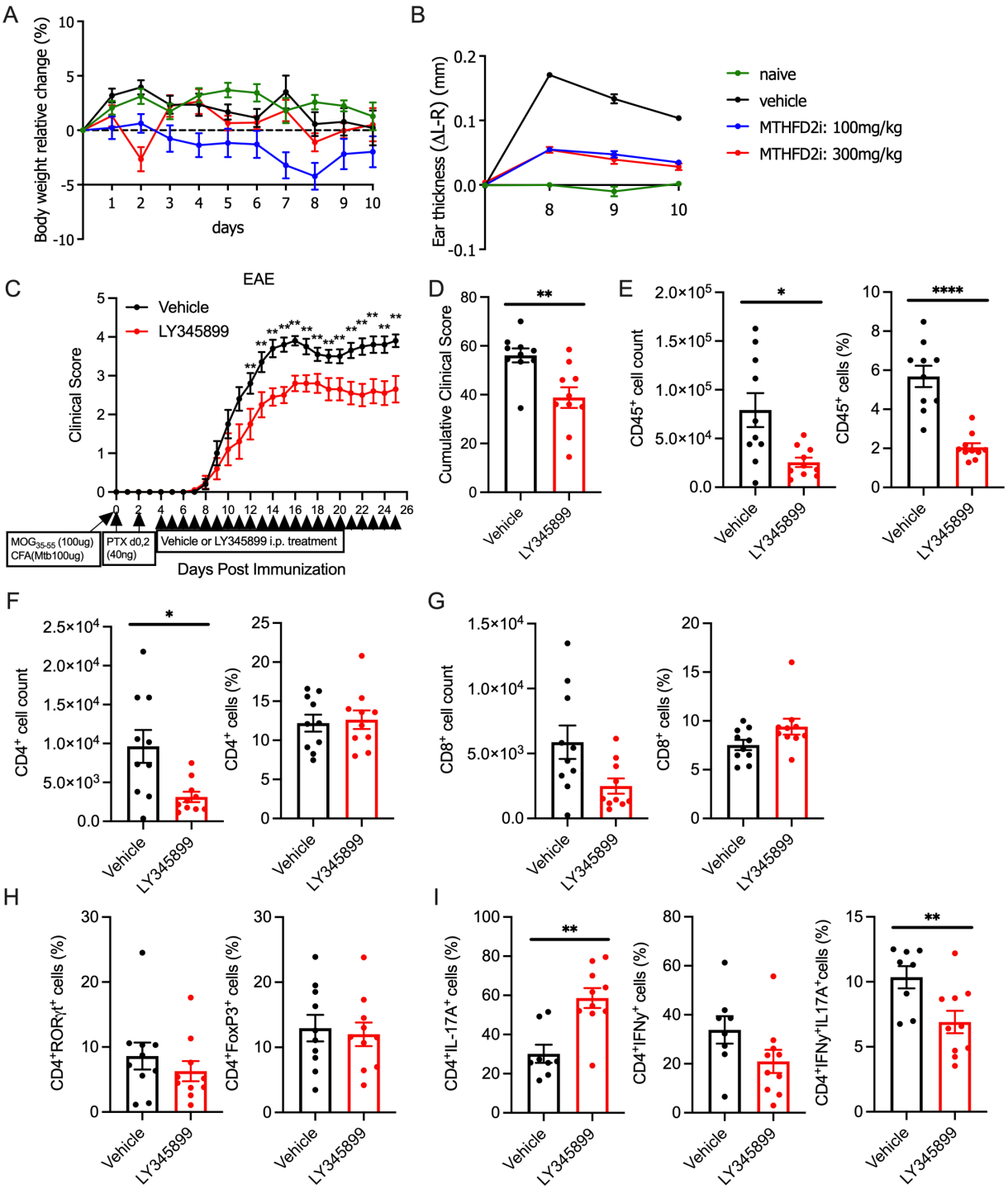

Figure S5: Effect of *in vivo* MTHFD2i treatment in DTH and EAE models. Related to Figure 7.

(A) Change in body weight from day 0 to 10 in mice immunized with KLH with CFA on day 0 and challenged with KLH on day 7, treated twice daily with oral vehicle, 100, or 300mg/kg MTHFD2i (mean±SEM, n=8). (B) Change in ear thickness from day 7 to 10 in the DTH mice from (A) (mean±SEM, n=8). Average (C) clinical score overtime and (D) and cumulative score in mice immunized with MOG with CFA and PTX to induce EAE and treated daily with i.p. vehicle or 10mg/kg LY345899 (mean±SEM, Mann-Whitney test, n=10). Cell count and frequency of (E) $CD45^+$, (F) $CD4^+$, and (G) $CD8^+$ cells in the spinal cord of EAE mice in (C) (mean±SEM, Mann-Whitney test). Frequency of (H) $ROR\gamma t^+$, $FoxP3^+$, (I) $IL\text{-}17^+$, $IFN\gamma^+$, and $IL\text{-}17^+IFN\gamma^+$ cells the spinal cord of EAE mice in (C) (mean±SEM, Mann-Whitney test).

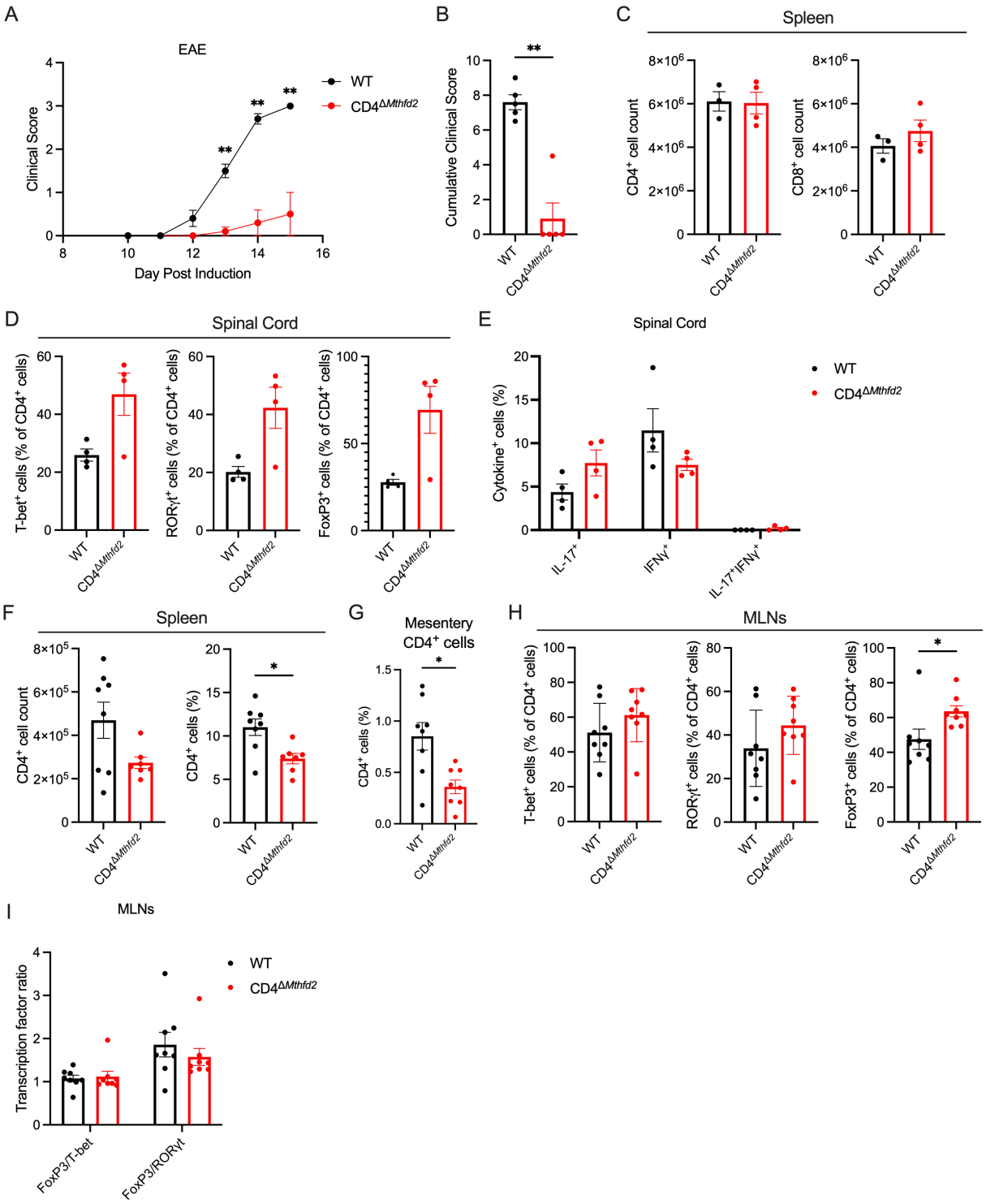

Figure S6: Effect of MTHFD2 loss *in vivo* in EAE and IBD models. Related to Figure 7.

Average (A) clinical score overtime and (B) cumulative score in WT and CD4$^{\Delta Mthfd2}$ littermates immunized with MOG with CFA and PTX to induce EAE (mean±SEM, multiple Mann-Whitney tests, n=5). Repeat of experiment in Figure 7D, halted at peak disease severity.
(C) CD4^{+} and CD8^{+} T cell count in the spleen of EAE mice from (A) (mean±SEM, Mann-Whitney test). Frequency of (D) T-bet^{+}, RORγt^{+}, FoxP3^{+}, (E) IL-17^{+}, IFNγ^{+}, and IL-17^{+}IFNγ^{+} cells in the spinal cord of EAE mice in (A) (mean±SEM, Mann-Whitney test). (F) CD4^{+} T cell count and frequency in the MLNs of IBD mice from Figure 7J (mean±SEM, Mann-Whitney test). (G) Frequency of CD4^{+} T cells within the mesentery of IBD mice from Figure 7J (mean±SEM, Mann-Whitney test). (H) Frequency of T-bet^{+}, RORγt^{+}, and FoxP3^{+} cells in the MLNs of IBD mice from Figure 7J (mean±SEM, Mann-Whitney test). (I) Ratio of FoxP3^{+} cell count to T-bet^{+} and RORγt^{+} cell counts in CD4^{+} T cells from the MLNs of IBD mice from Figure 7J (mean±SEM, Mann-Whitney test).

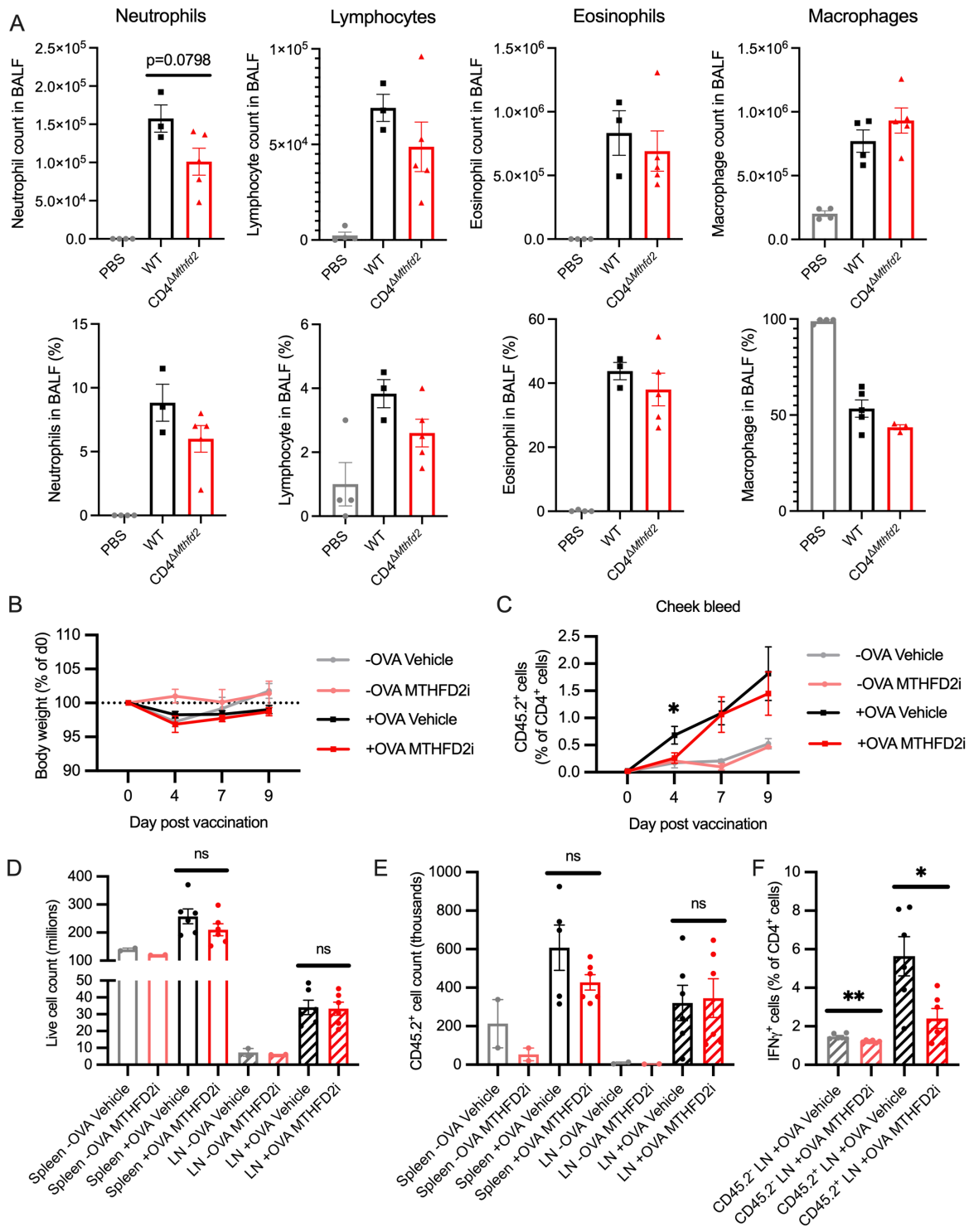

Figure S7: Effect of MTHFD2 deficiency *in vivo* in allergic airway disease and OT-II models. Related to Figure 7.

(A) Cell count and frequency of neutrophils, lymphocytes, eosinophils, and macrophages in BALF collected from WT and $CD4^{\Delta Mthfd2}$ mice sensitized with intranasal PBS or Alternaria Extract (mean±SEM, unpaired t-test). (B) Change in body weight from day 0 to 9 in CD45.1 mice adoptively transferred with 1 million OT-II $CD45.2^+$ $CD4^+$ T cells, immunized with OVA with CFA, and treated with daily oral vehicle or 300mg/kg MTHFD2i (mean±SEM, multiple unpaired t-tests, n=6). (C) Frequency of OT-II $CD45.2^+$ cells of total $CD4^+$ T cells isolated by cheek bleed in mice from (B) (mean±SEM, multiple unpaired t-tests, n=6). Counts of (D) total live cells and (E) OT-II $CD45.2^+$ cells isolated from spleen and draining LNs of mice from (B) (unpaired t-test). (F) Percentage of $IFN\gamma^+$ cells among $CD4^+CD45.2^-$ and $CD45.2^+$ T cells from draining LNs in mice from (B) (unpaired t-test).